Eur Biophys J (2010) 39:415–422
DOI 10.1007/s00249-009-0416-2

ORIGINAL PAPER

# Modulation of aggregate size- and shape-distributions of the amyloid-$\beta$ peptide by a designed $\beta$-sheet breaker

**Luitgard Nagel-Steger · Borries Demeler · Wolfgang Meyer-Zaika · Katrin Hochdörffer · Thomas Schrader · Dieter Willbold**

Received: 14 November 2008 / Revised: 26 January 2009 / Accepted: 2 February 2009 / Published online: 24 February 2009


**Abstract** A peptide with 42 amino acid residues (A$\beta$42) plays a key role in the pathogenesis of the Alzheimer's disease. It is highly prone to self aggregation leading to the formation of fibrils which are deposited in amyloid plaques in the brain of diseased individuals. In our study we established a method to analyze the aggregation behavior of the A$\beta$ peptide with a combination of sedimentation velocity centrifugation and enhanced data evaluation software as implemented in the software package UltraScan. Important information which becomes accessible by this methodology is the *s*-value distribution and concomitantly also the shape-distribution of the A$\beta$ peptide aggregates generated by self-association. With this method we characterized the aggregation modifying effect of a designed $\beta$-sheet breaker molecule. This compound is built from three head-to-tail connected aminopyrazole moieties and represents a derivative of the already described Tripyrazole. By addition of this compound to a solution of the A$\beta$42 peptide the maximum of the *s*-value distribution was clearly shifted to smaller *s*-values as compared to solutions where only the vehicle DMSO was added. This shift to smaller *s*-values was stable for at least 7 days. The information about size- and shape-distributions present in aggregated A$\beta$42 solutions was confirmed by transmission electron microscopy and by measurement of amyloid formation by thioflavin T fluorescence.

**Keywords** Sedimentation velocity centrifugation · Transmission electron microscopy · Thioflavin T · Amyloid $\beta$ peptide · Aggregation inhibitor · Alzheimer's disease

**Abbreviations**

| | |
|---|---|
| DMSO | Dimethylsulfoxide |
| PBS | Phosphate buffered saline |
| FITC | Fluorescein isothiocyanate |
| A$\beta$42 | Amyloid $\beta$ (1-42) peptide |
| A$\beta$40 | Amyloid $\beta$ (1-40) peptide |
| ThT | Thioflavin T |
| 2D-SA | 2-Dimensional spectrum analysis |
| GA | Genetic algorithm |
| Rmsd | Root mean square deviation |

AUC&HYDRO 2008—Contributions from 17th International Symposium on Analytical Ultracentrifugation and Hydrodynamics, Newcastle, UK, 11–12 September 2008.

L. Nagel-Steger (✉) · D. Willbold
Institute for Physical Biology, Geb.26.12.U1,
Heinrich-Heine University Düsseldorf,
Universitätsstrasse 1, 40225 Düsseldorf, Germany
e-mail: nagelst@biophys.uni-duesseldorf.de

B. Demeler
Department of Biochemistry, University of Texas Health Science Center at San Antonio, Floyd Curl Drive,
San Antonio, TX 7703, USA
e-mail: demeler@biochem.uthscasa.edu

W. Meyer-Zaika
Institute for Anorganic Chemistry, University Duisburg-Essen,
45117 Essen, Germany
e-mail: meyer-zaika@uni-due.de

K. Hochdörffer · T. Schrader
Institute for Organic Chemistry, University Duisburg-Essen,
45117 Essen, Germany

T. Schrader
e-mail: schrader@uni-due.de

D. Willbold
Institute for Structural Biology and Biophysics, ISB-3,
Research Centre Jülich, 52425 Jülich, Germany
e-mail: d.willbold@fz-juelich.de

RT Room temperature
TEM Transmission electron microscopy

## Introduction

The property of proteins to self-associate to highly ordered structures is of multiple interests since its discovery in the context of human neurodegenerative diseases, such as Parkinson's, Alzheimer's, Huntington's and prion diseases (reviewed in Chiti and Dobson 2006). One of the hallmarks in Alzheimer's disease is the formation of extracellular amyloid plaques consisting mainly of a proteolytic fragment of the amyloid precursor protein, the amyloid $\beta$ peptide. While at first the fibril was considered as the major culprit of disease symptoms, increasing evidence points to smaller oligomeric species (Selkoe 2008; Walsh and Selkoe 2007; Lesné et al. 2006; Lambert et al. 1998) as neurotoxic agents (Kirkidadze et al. 2002). The self-association of the amyloid $\beta$ peptide is therefore target for several therapeutic concepts (Spencer et al. 2007). Characterization of the end products of this process, the amyloid fibrils, as well as the characterization of other forms of aggregation reactions in the pathway to fibril formation, requires use of advanced methods for determining size- and shape distributions under solution conditions. Sedimentation velocity centrifugation offers decisive advantages by avoiding problems arising from matrix interactions in size-exclusion chromatography and from the fact that no size standards for calibration are needed since analytical ultracentrifugation is a first principle method.

The application of sedimentation velocity centrifugation for the analysis of amyloid oligomers and fibrils (Mok and Howlett 2006) encompasses preparative as well as analytical ultracentrifugation methods allowing the separation of different aggregate sizes, the measurement of hydrodynamic parameters as well as the determination of *s*-value distributions. Sedimentation velocity centrifugation was already applied to the determination of *s*-value distributions by different groups (Hepler et al. 2006; Lashuel et al. 2002; Seilheimer et al. 1997) to analyze self-association of the amyloid $\beta$ peptide. We expanded the method of sedimentation velocity centrifugation by applying advanced data analysis tools for the analysis of self-polymerizing amyloid $\beta$ solutions.

Based on the positive results obtained with designed $\beta$-sheet breaker molecules built from aminopyrazole moieties (Rzepecki et al. 2004; Kirsten and Schrader 1997) new derivatives of the trimeric aminopyrazole compound were synthesized and tested for their potential to inhibit the aggregation of the amyloid $\beta$ peptide. The pronounced effect of one derivative compound on the *s*-value distribution observed for an A$\beta$42 solution is the subject of this article. This compound referred to as test compound in the following sections is build out of three aminopyrazoles with a 5′ nitro group on one end and a 3′-carboxyl group on the other end.

## Materials and methods

The amyloid $\beta$ peptides (1-42) and (1-40) (Bachem, Bubendorf, Germany) were predissolved in 2 mM NaOH (Fezoui et al. 2000). After freeze-drying aliquots were stored at −70°C until use. FITC-Ala-amyloid $\beta$-protein (1-42) was purchased from Bachem (Bubendorf, Germany) or alternatively A$\beta$42 N-terminally labeled with the dye Oregon Green™ (A$\beta$42-OG) was synthesized by P. Henklein (Charité, Berlin, Germany). Labeled peptides were predissolved in 100% anhydrous dimethylsulfoxide (DMSO) and stored as aliquots at −70°C. The test compound was dissolved in 100% anhydrous DMSO; 5 mM stock solutions were stored at 4°C.

### Thioflavin T fluorescence assay

Thioflavin T (ThT) fluorescence measurements were performed in a 384-well plate (Nunc GmbH, Wiesbaden, Germany) in a Tecan Safire plate reader (Tecan GmbH, Crailsheim, Germany). Fluorescence was measured at 37°C, 446 nm excitation and 490 nm emission wavelengths with 2.5 nm bandwidth and constant gain. Each data point was averaged over 10 lamp flashes. Prior to each measurement the optimal z-position was manually determined. Measurement cycles were started by shaking the sample carrier orbitally for 30 s at medium intensity to avoid settling of larger aggregates. A sample was composed of 33 μM A$\beta$40 in 10 mM phosphate buffered saline (PBS), 6% DMSO, 10 μM ThT either with 330 μM test compound or the vehicle DMSO alone. Fluorescence emission at 490 nm was determined every hour during the incubation period. For graph representation emission values of triplicate samples were averaged. Test compound alone was measured in the same buffer to exclude any effects upon ThT fluorescence detection.

### Sedimentation velocity centrifugation

Sedimentation velocity centrifugation was performed in an XL-A (Beckman-Coulter, Palo Alto, USA) equipped with absorption optics and a four-hole titanium rotor. Prior to the centrifugation the solutions were incubated slightly agitated at room temperature for different incubation times. Sample volumes ranging from 300 to 400 μl were filled into standard double sector aluminum center pieces and

spun at 20,000 rpm, 20°C after thermal calibration. Radial scans were recorded at a resolution of 0.002 cm. Detection wavelength was chosen at 493 nm to observe end-labeled FITC or Oregon Green™ and to avoid background absorbance from the test compound.

### Data analysis

Sedimentation data were analyzed with UltraScan 9.4 (http://www.ultrascan.uthscsa.edu). After time-invariant noise subtraction, *s*-value distributions were determined model independently using the enhanced van Holde-Weischet method in the UltraScan software (Demeler and van Holde 2004; van Holde and Weischet 1978). Molecular weight and frictional ratios were determined with two-dimensional spectrum analysis (Brookes et al. 2006) and the genetic algorithm optimization method (Brookes and Demeler 2006, 2007). Hydrodynamic corrections for buffer conditions were made according to data published by Laue et al. (1992) as implemented in UltraScan. The partial specific volume of the A$\beta$42 $\bar{\nu} = 0.7377 \mathrm{cm}^3/\mathrm{g}$ was calculated on the basis of its amino acid content by a routine implemented in UltraScan. Experimental intensity data were time-invariant noise corrected using the 2D-SA analysis. The van Holde–Weischet analysis was used to initialize the *s*-value range in the 2D-SA from 1 to 150 S. The frictional ratio range was initialized between 1 and 10. 2D-SA analyses were performed with 24 grid movings with a 10 point resolution in both dimensions, resulting in a final *s*-value resolution of 0.625 S and 0.042 $f/f_0$ units. The 2D-SA results were used to initialize the GA analysis, and parsimoniously regularized GA distributions were used to initialize the GA Monte Carlo analysis. Data were analyzed on the Bioinformatics Core Facility cluster (University of Texas, Health Science Center, San Antonio, TX, USA) and on the Lonestar cluster at the Texas Advanced Computing Center (Austin, TX, USA). The hydrodynamic behavior of a molecule sedimenting in a sector shaped cell is fully described by the Lamm equation (Lamm 1929). In the case of polydisperse samples the shape of the sedimentation boundary and its evolution over time contains information about size, shape and partial concentration of the sedimenting species. To extract the information a linear combination of solutions of the Lamm equation is fitted to the experimental data. The simulated solutes represented in the linear combination of Lamm equations cover both the sedimentation coefficient range as well as the frictional ratio range of solutes present in the experimental data.

### Transmission electron microscopy (TEM)

TEM experiments were performed with a Phillips CM 200 FEG instrument. After absorbing 5 µl of a tenfold diluted sample of the solution used for analytical ultracentrifugation to the holey carbon film coated copper grids (Plano, Wetzlar, Germany) the samples were washed twice with 0.1 and 0.01 mM ammonium acetate and then negatively stained with 2% (w/v) ammonium molybdate solution for 90 s.

## Results

A standard test for amyloid formation is the Thioflavin T (ThT) assay (LeVine 1999; Naiki et al. 1989). ThT changes its fluorescence properties upon binding to amyloid, by a shift in the emission wavelength and an increase in quantum yield. Figure 1 shows the ThT fluorescence measured hourly over 76 h for A$\beta$40, A$\beta$40 with a tenfold molar excess of test compound and test compound alone. ThT fluorescence increased over time upon incubation of A$\beta$40 (diamonds), thus indicating the aggregation of A$\beta$40. Addition of the test compound led to a 50% reduced ThT fluorescence after 76 h of incubation at 37°C, as compared to the control reaction where only the vehicle DMSO was added. No fluorescence was detected for the test compound alone at the assay conditions. This indicated a possible aggregation inhibition property of the compound.

Since the ThT fluorescence measurements can be affected adversely by competitive binding of the compound to the binding places of ThT, the drug-amyloid interaction needed further characterization. Inhibition of amyloid formation should be measured directly by a changed aggregation state of mixtures containing the compound compared to control mixtures. For this purpose sedimentation velocity centrifugation experiments were performed. The solution conditions were optimized to minimize the formation of large aggregates by choosing low salt concentrations. Ideally every aggregate present in solution should remain soluble and thus measurable during the experiment. But also in those cases where this was not achievable, at least the loss of material in form of insoluble aggregates, which sediment during acceleration and early scans of the experiment, could be quantified.

Figure 2 shows sedimentation velocity data for a solution of 70 µM A$\beta$42, 14 µM A$\beta$42-FITC incubated for 5 h, 1, 2 and 5 days. The corresponding extrapolation plots according to van Holde and Weischet (1978) are shown below the raw data. By extrapolation to infinite time it is possible to separate the diffusion information from the sedimentation properties of the sample. For an ideal 1-component system the lines would intercept the *y*-axis in one point, which marks the diffusion corrected *s*-value. The presence of numerous intercepts in the depicted plots indicates the degree of heterogeneity of the sample. The weight average *s*-value of the particles remaining soluble

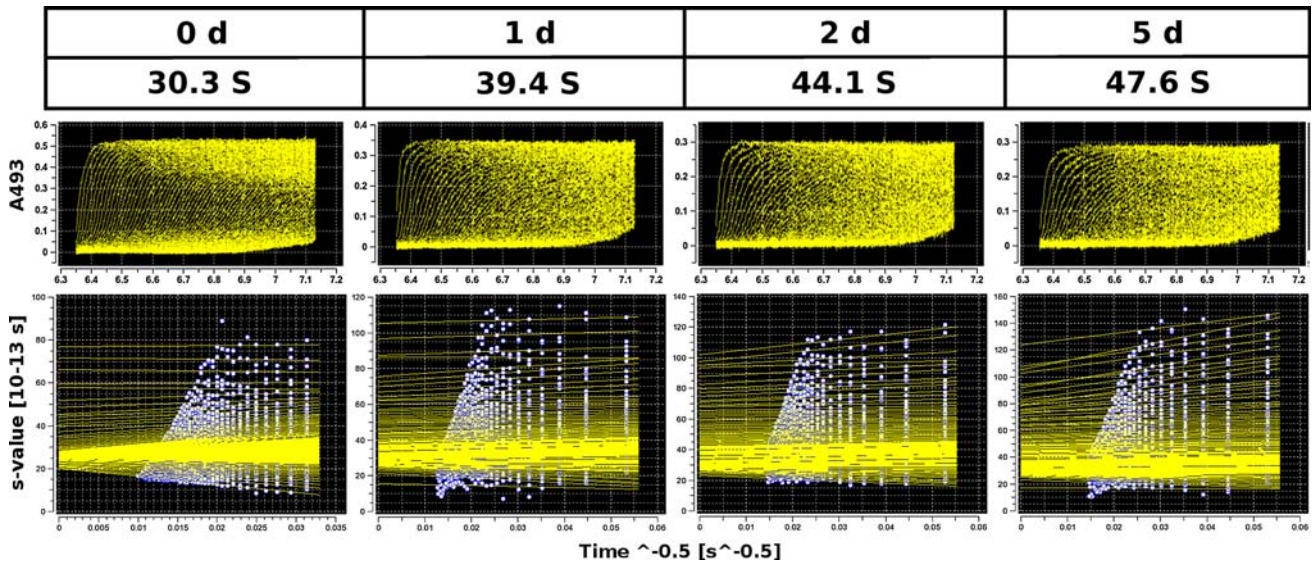


**Fig. 1** Sedimentation profiles of A$\beta$42 incubated for 0, 1, 2, 5 days with corresponding van Holde–Weischet extrapolation plots and the calculated weight average sedimentation coefficients. About 70 μM A$\beta$42/14 μM A$\beta$42-FITC in 10 mM sodium phosphate buffer, pH 7.4, 8% DMSO were centrifuged at 20,000 at 20°C after incubation slowly agitated at room temperature for the indicated times

during the incubation period increased from 30.3 to 47.6 S ($10^{-13}$ s) documenting the growth of A$\beta$ aggregates over time. The weight-average sedimentation coefficients are calculated from the weighted sum of all species in the 2DSA grid that were returned with positive, non-zero amplitudes by the NNLS (non-negative least squares fit). According to the boundary height determined by extrapolation to zero time only 55% of the peptide remained soluble at day 5. This high loss could be markedly reduced by decreasing the amyloid peptide concentration in further experiments.

Figure 3 shows the sedimentation profiles collected for samples with and without added compound after 5 days of incubation. Measuring in intensity instead of absorption mode allowed for a reduction of amyloid $\beta$ peptide concentration to 21 μM (17.5 μM A$\beta$42 and 3.5 μM A$\beta$42-OG) without a loss in signal quality. The collected sedimentation profiles of the two samples differ clearly from each other indicating a reduced sedimentation velocity of the peptide as consequence of the added test compound. For both measurements the loading concentration determined by extrapolation to zero time by the van Holde–Weischet procedure of UltraScan matched well the spectroscopically measured concentration prior to incubation and centrifugation. The loss due to insoluble material after 5 days incubation amounted 8% in the control and less than 1% in the compound containing sample. Analysis of the data by the 2-dimensional spectrum analysis (2D-SA) and the genetic algorithm (GA) based analysis methods revealed the composition of the samples with regard to size and shape of the formed A$\beta$ aggregates and their partial

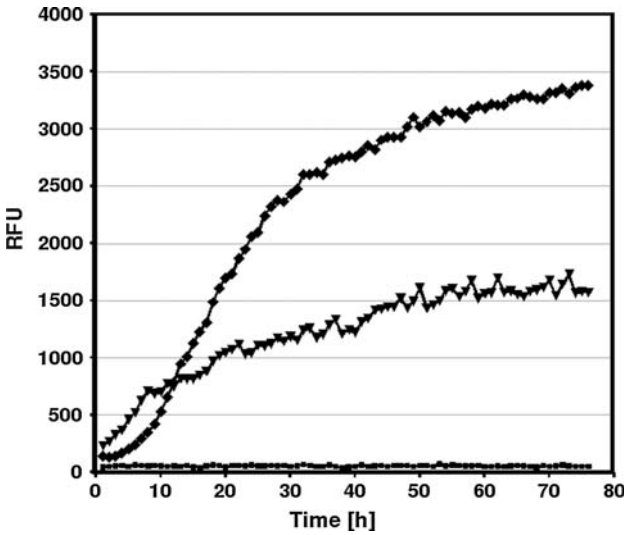


**Fig. 2** Thioflavin T fluorescence assay of test compound: 33 μM A$\beta$40 in 1× PBS with 6% DMSO (*diamonds*) with 330 μM test compound (*triangles*) and test compound alone (*squares*). Each data point is the mean of a triplicate assay

concentration. After removal of the time invariant noise in the course of the 2D-SA a preliminary distribution of species is found giving weight average values for *s*-value, molecular weight and diffusion coefficient (cf. Table 1). These values are used to initialize the GA analysis. Its solution was probed by Monte Carlo statistics to give the final result. The test compound reduced the sedimentation coefficient of the pure A$\beta$ distribution from 52 to 25.5 S. This decrease is only partly a consequence of a reduced molecular weight; an increase of the frictional ratio

**Table 1** Results from UltraScan data analysis for A$\beta$42 without and with test compound: weight average values for the *s*-value, molecular weight and diffusion coefficient, as determined by 2-dimensional spectrum analysis (2D-SA), genetic algorithm based analysis (GA) and GA tested by Monte Carlo statistics (GA–MC)

| | A$\beta$42 | | | | A$\beta$42 with 200 μM test compound | | | |
|---|---|---|---|---|---|---|---|---|
| | *s*-value ($10^{-13}$ s) | MW (g/mol) | *D* ($cm^2$/s) | rmsd | *s*-value ($10^{-13}$ s) | MW (g/mol) | *D* ($cm^2$/s) | rmsd |
| 2D-SA | 52.4 | $1.25 \cdot 10^7$ | $1.39 \cdot 10^{-7}$ | 0.0026 | 25.3 | $5.18 \cdot 10^6$ | $1.32 \cdot 10^{-7}$ | 0.0031 |
| GA | 52.0 | $4.78 \cdot 10^6$ | $1.58 \cdot 10^{-7}$ | 0.0026 | 25.5 | $1.99 \cdot 10^6$ | $1.08 \cdot 10^{-7}$ | 0.0033 |
| GA–MC | 52.0 | $2.81 \cdot 10^6$ | $2.10 \cdot 10^{-7}$ | 0.0027 | 25.5 | $1.99 \cdot 10^6$ | $2.06 \cdot 10^{-7}$ | 0.0034 |

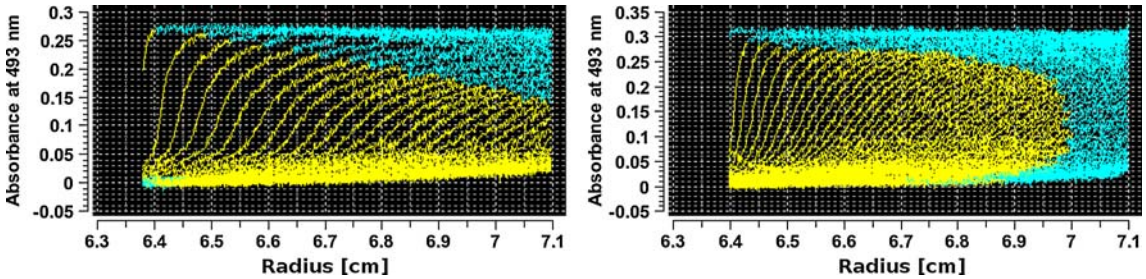


**Fig. 3** Sedimentation profiles taken at 5 min interval during centrifugation at 20,000 rpm, 20°C. *Left* 21 μM A$\beta$42/A$\beta$42-OG without test compound, 5 days incubation at RT. *Right* 21 μM A$\beta$42/A$\beta$42-OG with 200 μM test compound, 5 days incubation at RT

considerably contributes to the *s*-value reduction. The addition of the test compound led to a 60% reduced weight average molecular weight. Table 1 summarizes the weight average values for sedimentation coefficient, molecular weight and diffusion coefficient obtained from the different data evaluation procedures. The rmsd value in the last column indicates the good quality of the fits.

The GA analysis validated by Monte Carlo statistics does not only allow for an evaluation of the sedimentation data in terms of weight average values but also in terms of species numbers and their individual characteristics. In Fig. 4 the *s*-values of the solutes are plotted versus their corresponding frictional ratio in the *x*–*y* plane, while their partial concentration is plotted color coded in the pseudo-third dimension (Brookes and Demeler 2006). A solute with 53 S and a frictional ratio of 1.8 is the dominant species (34.8%) in the control sample with only A$\beta$42/A42-OG. Also globular species are found. In the A$\beta$42/A$\beta$42-OG sample when test compound was added, solutes with *s*-values larger than 45 S are missing. New species with *s*-values of 22 S (74.4% between 16.4 and 28.1 S) appear with increased, not clearly defined frictional ratios. Table 2 lists the *s*-values of globular species found in the control sample with their corresponding frictional ratio, relative concentration, molecular weight and calculated diameter. Two of these five species, the 28.7 and the 46.4 S species, are detected in the samples without test compound: one species of 28.1 S with a relative fraction of 24.4% and

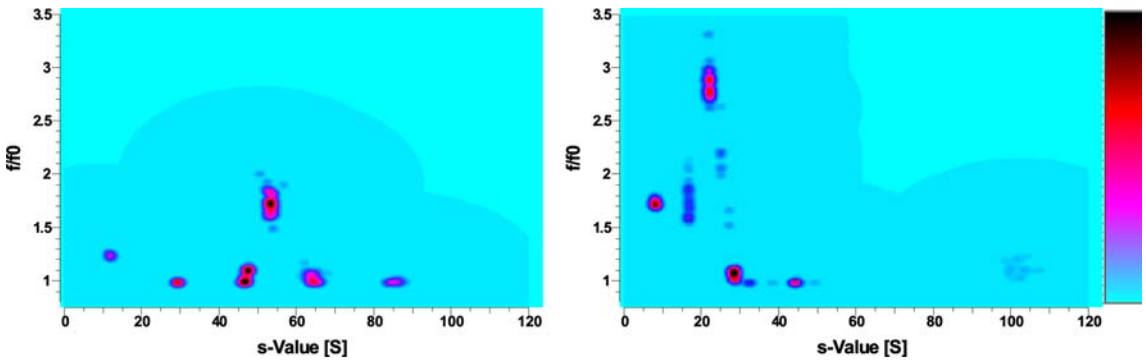


**Fig. 4** Graphical representation of species detected by GA–MC analysis with *s*-value and frictional ratio in pseudo-3D plots. *Left* 21 μM A$\beta$42/A$\beta$42-OG without test compound. *Right* 21 μM A$\beta$42/A$\beta$42-OG with 200 μM test compound. Samples were incubated slowly agitated for 5 days at RT prior to centrifugation. An obvious decrease in the concentration of larger, globular structures is observed when test compound is added, favoring smaller species with larger frictional coefficients

**Table 2** Globular species detected by sedimentation velocity centrifugation of A$\beta$42 and their calculated diameter (calculations were done according to van Holde et al. 2006)

| *s*-value ($10^{-13}$ s) | $f/f_0$ | Relative concentration (%) | Calc. diameter (nm) | MW (g/mol) |
|---|---|---|---|---|
| 11.5 | 1.2496 | 4.20 | 4.3 | $2.7 \cdot 10^5$ |
| 28.7 | 1.0002 | 7.90 | 12.0 | $7.5 \cdot 10^5$ |
| 46.4 | 1.0017 | 27.80 | 15.5 | $1.5 \cdot 10^6$ |
| 65.2 | 1.0019 | 17.90 | 18.2 | $2.6 \cdot 10^6$ |
| 84.0 | 1.0004 | 7.39 | 20.7 | $3.8 \cdot 10^6$ |

Predicted sizes correlate well to the measured particles in TEM images

one of 43.8 S with 7.4%. Frictional ratios in our methods are constrained to fixed limits; the lower limit is constrained to be 1.0. This can be interpreted to mean "globular shape". Due to experimental noise, these values cannot be considered to be absolute and also have a certain error associated with them, which is determined in the GA-Monte Carlo method.

To complement these results measured in the sedimentation velocity centrifugation experiments an aliquot from each sample was analyzed by transmission electron microscopy (TEM). In Fig. 5a a TEM image of the A$\beta$ sample analyzed by sedimentation velocity centrifugation is shown. It contains mainly amyloid fibrils with the typical width of 10 nm, lengths reaching more than 500 nm and a helical twist of about 100 nm. Besides these mature fibrils (Antzutkin et al. 2002; Nybo et al. 1999) different kinds of globularly shaped particles could be detected. Globular particles ranging in diameter from 18 to 30 nm as shown in Fig. 5b as well as rather small particles visible only due to high resolution TEM of 3–4 nm diameter (Fig. 5c) were found in different image sections of the same grid. TEM images of the sample with the test compound showed reproducibly a reduced number of mature fibrils as compared to the control sample in combination with numerous thinner filaments, which are neither detectable in the pure A$\beta$42 samples nor in samples where the test compound was incubated alone for 5 days. These thinner filaments have a width of about 5 nm. Length estimates were hampered by the dense packing of these filaments.

## Discussion

The test compound was designed to recognize $\beta$-sheet conformation of amyloid formed by the A$\beta$ peptide. Decoration of open edges of growing $\beta$-sheets with bound test

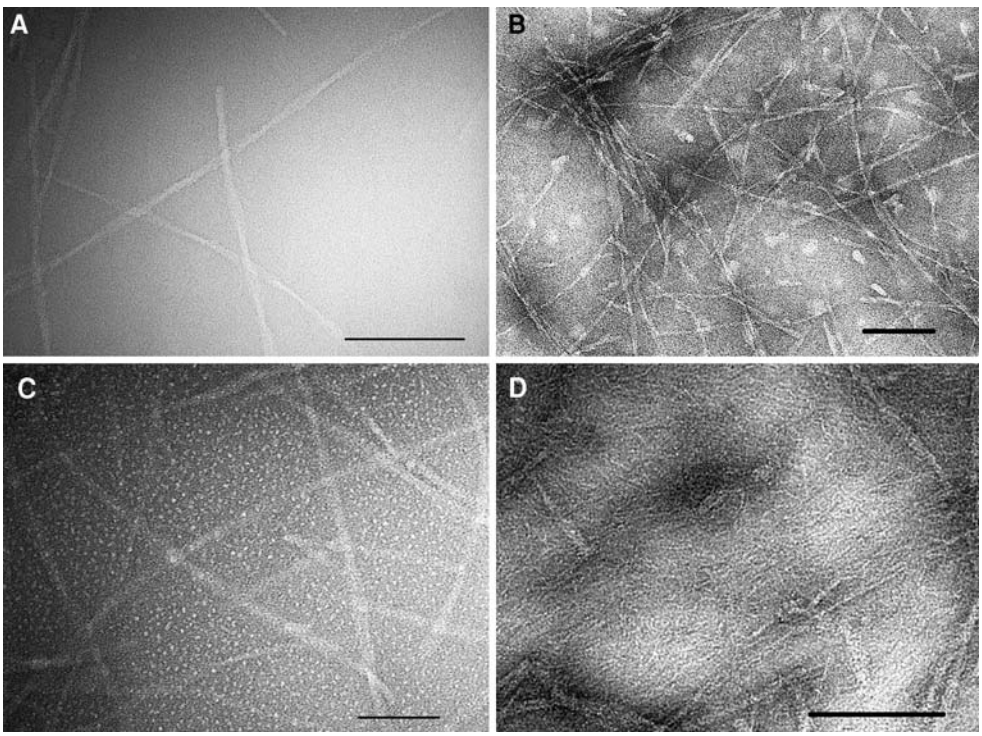


**Fig. 5** TEM images. **a** Image of A$\beta$42/A$\beta$42-OG showing mature fibrils with a periodicity of 100 nm. *Bar* 100 nm. **b** Electron micrograph of A$\beta$42 fibrils seen together with larger globular and elongated oligomers after 5 days of incubation slowly agitated at RT. *Bar* 100 nm. **c** Electron micrograph of A$\beta$42 fibrils seen together with small globular oligomers after 5 days of incubation slowly agitated at RT. High-resolution TEM with 135 kV. *Bar* 50 nm. **d** Electron micrograph of 21 µM A$\beta$42/A$\beta$42-OG mixed with 200 µM inhibitor after 5 days of incubation slowly agitated at RT. *Bar* 100 nm

compound should block further addition of A$\beta$ molecules. As a consequence a reduced size of aggregates should be expected. This expectation was fulfilled by the finding of a clearly reduced weight average *s*-value for A$\beta$ solutions incubated in the presence of the test compound. By enhanced data analysis the reduced *s*-value could be also attributed to a reduced weight average molecular weight of aggregates. TEM analysis of the samples used for analytical ultracentrifugation confirmed the striking difference between A$\beta$42 alone and A$\beta$42 incubated with test compound. No shortened fibrils, but large amounts of thin filaments were accumulated in the presence of the test compound, pointing to a disturbed lateral association of filaments. This correlates well with the increased frictional ratio calculated for the dominant species of A$\beta$ samples containing test compound and confirms the potency of the data evaluation method. Globular particles as predicted by the data analysis of the sedimentation velocity centrifugation experiments could also be verified by TEM. Their appearance during the aggregation of amyloid $\beta$ peptide is also documented in the literature (Hepler et al. 2006; Sabaté and Estelrich 2005; Seilheimer et al. 1997).

Due to recent findings regarding the nature of the toxic species (Rahimi et al. 2008; Selkoe 2008) responsible for the pathology of protein misfolding diseases, it is evident that a sole quantification of the amyloid content is not sufficient to ascertain the toxicity of a solution of a self-associating protein. Additional information about the sizes, shapes and partial concentrations of different forms of the disease related protein is highly desirable. The characterization of differently treated protein preparations, the monitoring of aggregation over time, and the investigation of modulators of the aggregation, as presented here, are examples for possible applications of the highly versatile method of sedimentation velocity centrifugation. Especially in the process of drug development targeting the aggregation of a disease related protein this information could be useful before proceeding from in vitro to in vivo experiments. ThT assay results might be skewed by problems arising from sample precipitation or competitive binding of the test compound. Analysis by ultracentrifugation does not depend on the binding of a dye molecule and allows controlling the loss of protein due to insoluble aggregates. It gives information directly about the *s*-value distribution of a sample. The determination of size- and shape-distributions of solutions of a disease related protein allows discriminating between different modes of action of test compounds, also necessary for the determination of structure-function relationships.

The method of sedimentation velocity centrifugation in conjunction with the presented data evaluation method is a powerful tool to study the aggregation process of amyloidogenic proteins.

**Acknowledgments** We would like to thank Bernd Esters for his skillful technical assistance. Computing time and computational support was provided by Texas Advanced Computing Center from UT Austin (NSF Teragrid Allocation grant TGMCB070038). We gratefully acknowledge support from the National Science Foundation through Teragrid grant TG-MCB060019T, as well as the National Institutes of Health through grant RR022200 (both to B.D.). L.N.S. was supported by a grant of the Volkswagenstiftung (I/82 649) in the priority area "interplay between molecular conformations and biological function".

## References

Antzutkin ON, Leapman RD, Balbach JJ, Tycko R (2002) Supramolecular structural constraints on alzheimer's $\beta$-amyloid fibrils from electron microscopy and solid-state nuclear magnetic resonance. Biochemistry 41:15436–15450. doi:10.1021/bi0204185

Brookes E, Demeler B (2006). Genetic algorithm optimization for obtaining accurate molecular weight distributions from sedimentation velocity experiments. In: Wandrey C, Cölfen H (eds) Analytical ultracentrifugation VIII. Progr Colloid Polym Sci 13:78–82

Brookes, E and Demeler, B. (2007). Parsimonious regularization using genetic algorithms applied to the analysis of analytical ultracentrifugation experiments. ACM GECCO proceedings 978-1-59593-697-4/07/0007

Brookes E, Boppana RV, Demeler B (2006). Computing large sparse multivariate optimization problems with application in biophysics. Supercomputing 2006. (http://sc06.supercomputing.org/schedule/pdf/pap320.pdf)

Chiti F, Dobson CM (2006) Protein misfolding, functional amyloid and human disease. Annu Rev Biochem 75:333–366. doi:10.1146/annurev.biochem.75.101304.123901

Demeler B, van Holde KE (2004) Sedimentation velocity analysis of highly heterogeneous systems. Anal Biochem 335:279–288. doi:10.1016/j.ab.2004.08.039

Fezoui Y, Hartley DM, Harper JD, Khurana R, Walsh DM, Condron MM, Selkoe DJ, Lansbury PT Jr, Fink AL, Teplow DB (2000) An improved method of preparing the amyloid $\beta$-protein for fibrillogenesis and neurotoxicity experiments. Amyloid 7:166–178. doi:10.3109/13506120009146831

Hepler RW, Grimm KM, Nahas DD, Breese R, Dodson EC, Acton P et al (2006) Solution state characterization of amyloid $\beta$-derived diffusible ligands. Biochemistry 45:15157–15167. doi:10.1021/bi061850f

Kirkidadze MD, Bitan G, Teplow DB (2002) Paradigm shifts in Alzheimer's disease and other neurodegenerative disorders: the emerging role of oligomeric assemblies. J Neurosci Res 69:567–577. doi:10.1002/jnr.10328

Kirsten C, Schrader T (1997) Intermolecular $\beta$-sheet stabilization with aminopyrazoles. J Am Chem Soc 119:12061–12068. doi:10.1021/ja972158y

Lambert MP, Barlow AK, Chromy BA, Edwards C, Freed R, Liosatos E et al (1998) Diffusible, nonfibrillar ligands derived from A$\beta$(1-42) are potent central nervous system neurotoxins. Proc Natl Acad Sci USA 95:6448–6453. doi:10.1073/pnas.95.11.6448

Lamm O (1929) Die Differentialgleichung der Ultrazentrifugierung. Ark Mater Astron Fys 21B:1–4

Lashuel HA, Hartley DM, Balakhaneh D, Aggarwal A, Teichberg S, Callaway DJE (2002) New class of inhibitors of amyloid-$\beta$ fibril formation. J Biol Chem 277:42881–42890. doi:10.1074/jbc.M206593200

Laue T, Shah B, Ridgeway T, Pelletier S (1992). Computer-aided interpretation of analytical sedimentation data for proteins.

Analytical ultracentrifugation in biochemistry and polymer science. The Royal Society of Chemistry, Cambridge, pp 90–125

Lesné S, Koh MT, Kotilinek L, Kayed R, Glabe CG, Yang A, Gallagher M, Ashe KH (2006) A specific amyloid-$\beta$ protein assembly in the brain impairs memory. Nature 440:352–357. doi:10.1038/nature04533

LeVine H (1999) Quantification of $\beta$-sheet amyloid fibril structures with thioflavin T. Methods Enzymol 309:274–284. doi:10.1016/S0076-6879(99)09020-5

Mok Y-F, Howlett GJ (2006) Sedimentation velocity analysis of amyloid oligomers and fibrils. Methods Enzymol 413:199–217. doi:10.1016/S0076-6879(06)13011-6

Naiki H, Higuchi K, Hosokava M, Takeda T (1989) Fluorometric determination of amyloid fibrils in vitro using the fluorescent dye, thioflavin T1. Anal Biochem 177:244–249. doi:10.1016/0003-2697(89)90046-8

Nybo M, Svehag SE, Holm Nielsen E (1999) An ultrastructural study of amyloid intermediates in A$\beta$1-42 fibrillogenesis. Scand J Immunol 49:219–223. doi:10.1046/j.1365-3083.1999.00526.x

Rahimi F, Shanmugam A, Bitan G (2008) Structure-function relationships of pre-fibrillar protein assemblies in Alzheimer's disease and related disorders. Curr Alzheimer Res 5:319–341. doi:10.2174/156720508784533358

Rzepecki P, Nagel-Steger L, Feuerstein S, Linne U, Molt O, Zadmard R, Aschermann K, Wehner M, Schrader T, Riesner D (2004) Prevention of Alzheimer's associated A$\beta$-aggregation by rationally designed nonpeptidic $\beta$-sheet ligands. J Biol Chem 279:47497–47505. doi:10.1074/jbc.M405914200

Sabaté R, Estelrich J (2005) Evidence of the existence of micelles in the fibrillogenesis of A$\beta$-amyloid peptide. J Phys Chem B 109:11027–11032. doi:10.1021/jp050716m

Seilheimer B, Bohrmann B, Bondolfi L, Müller F, Stüber D, Döbeli H (1997) The toxicity of the Alzheimer's $\beta$-amyloid peptide correlates with a distinct fiber morphology. J Struct Biol 119:59–71. doi:10.1006/jsbi.1997.3859

Selkoe DJ (2008) Soluble oligomers of the amyloid $\beta$-protein impair synaptic plasticity and behaviour. Behav Brain Res 192:106–113. doi:10.1016/j.bbr.2008.02.016

Spencer B, Rockenstein E, Crews L, Marr R, Masliah E (2007) Novel strategies for Alzheimer's disease treatment. Expert Opin Biol Ther 7:1853–1867. doi:10.1517/14712598.7.12.1853

Van Holde KE, Weischet WO (1978) Boundary analysis of sedimentation velocity experiments with monodisperse and paucidisperse solutes. Biopolymers 17:1387–1403. doi:10.1002/bip.1978.360170602

Van Holde KE, Johnson WC, Ho PS (2006). Principals of physical biochemistry, 2nd edn. Prentice-Hall, Englewood, pp 230–231. (ISBN 0-13-201744-X)

Walsh DM, Selkoe DJ (2007) A$\beta$ oligomers—a decade of discovery. J Neurochem 101:1172–1184. doi:10.1111/j.1471-4159.2006.04426.x